論文の内容の要旨

論文題目

Study on Epitaxial Perovskite Li-ion Conducting Thin Films: Strain-controlled Ionic Conduction and Heterostructure

(ペロブスカイト型Liイオン伝導体エピタキシャル薄膜の研究: 歪制御イオン伝導とヘテロ構造)

韋　嶸（WEI　Jie）
ウィ　ジェイ

1. Introduction

Solid electrolyte lithium lanthanum titanate $Li_{3x}La_{2/3-x}TiO_3$ (LLT, $0.05 < x < 0.167$) with A-site vacant perovskite structure (Figure 1a) shows the highest ionic conductivity up to 1 mS/cm at room temperature [1], which is comparable to those in conventional organic solvent electrolytes, thus attracts great interests. Since grain boundaries significantly suppress the Li ionic conductivity in bulk LLT specimens, single crystal sample is required, however difficult to obtain in bulk study. Recently, epitaxial thin film growth of LLT by pulsed laser deposition (PLD) attracted many interests to prepare single crystal specimens. The problem is that Li-loss was significant in previous epitaxial thin film studies and strangle further property investigation.

In this dissertation, Li-rich LLT target in PLD process was used in order to compensate the Li-loss observed in the previous experiment. Also, laser fluence was varied in addition to temperature and oxygen pressure of PLD process to control Li-composition precisely. By optimizing the laser fluence, highly crystalline LLT thin film with stoichiometric composition was obtained, enabling the measurement of intrinsically high ionic conduction. In addition, the magnitude of epitaxial strain was varied by using different perovskite substrates and strain-controlled ionic conduction under atmospheric condition was demonstrated. Moreover, LLT heteroepitaxial structure was formed on $La_{0.6}Sr_{0.4}MnO_3$ (LSMO) bottom electrode layer as a preliminary study toward all solid state heteroepitaxial Li-ion battery.

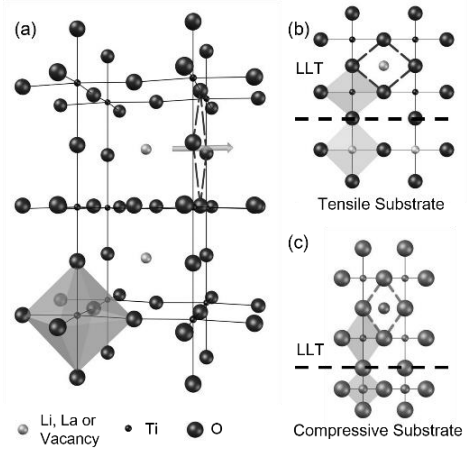

Figure 1 (a) Schematic crystal structure of LLT and epitaxial thin film with tensile (b) and compressive (c) strains.

2. Fabrication of epitaxial LLT thin film and strain-controlled ionic conductivity

From the demand for highly crystalline LLT thin film, PLD method was applied in several pioneering studies [2, 3]. However, most of them faced low ionic conductivity due to Li-loss in the films. In this dissertation, phase pure stoichiometric $Li_{0.33}La_{0.56}TiO_3$ thin film was fabricated by compensating Li-loss with a Li-rich target and by varying laser fluence. In addition, tensile and

compressive strains are expected to control the size of LLT cell, i.e., the bottleneck size of Li diffusion path (dashed diamond in Figure 1b, c). Therefore, it is expected to obtain artificially controllable ionic conductivity in atmospheric condition by strain. Here, tensile and compressive strains were applied by various mismatched substrates. Strain-controlled LLT ionic conductivity was observed in LLT thin film on orthorhombic $NdGaO_3$ (110) substrate for the first time.

Experiment

LLT thin films were fabricated by PLD method from a Li-rich target $Li_{0.84}La_{0.56}TiO_{3+\delta}$ synthesized by solid state reaction. Cubic $SrTiO_3$ (100) (STO), cubic $(LaAlO_3)_{0.3}$-$(SrAl_{0.5}Ta_{0.5}O_3)_{0.7}$ (100) (LSAT), and orthorhombic $NdGaO_3$ (110) (NGO) single crystals were chosen as substrates. KrF excimer laser fluence of PLD was varied from 0.5 to 2 J/cm^2 by a half-wave attenuator and frequency was fixed as 10 Hz. Crystal structures were analyzed by X-ray diffraction (XRD) and surface morphology was observed by atomic force microscopy. Several Ti/Au comb-type electrodes with length/width of 5900 μm/20 μm were patterned on LLT thin film by photolithography and deposited by ultrahigh vacuum deposition. Ionic conductivity of LLT thin films was measured by ac impedance analyzer in a probe system based with the comb electrodes. LLT thin film was dissolved into HNO_3/HCl mixture and its composition was analyzed by inductively coupled plasma emission spectrometry and flameless graphite furnace atomic absorption spectroscopy.

Results and Discussion

Figure 2 shows out-of-plane 2θ–θ patterns of LLT thin films under different laser fluence on LSAT (100) substrates with fixed substrate temperature and oxygen pressure. At lower laser fluence of 1.2 and 1.3 J/cm^2, Li-rich spinel $Li_4Ti_5O_{12}$ impurity appeared, while pyrochlore $La_2Ti_2O_7$ impurity appeared at higher laser fluence of 1.5 J/cm^2. Only at intermediate 1.4 J/cm^2, phase pure $Li_{0.33}La_{0.56}TiO_3$ phase was obtained as determined by composition analysis. This indicates that Li-composition decreased with increasing laser fluence, possibly due to the stronger re-sputtering and expanded plume effect on light Li than much heavier La and Ti. Low laser fluence prevents Li deficiency in thin film but significantly decreases the growth rate, resulting in insufficient film thickness. Therefore, Li-rich LLT target was used to obtain stoichiometric LLT film with a high growth rate.

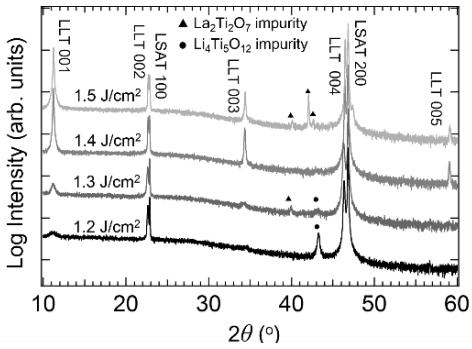

Figure 2 Out-of-plane 2θ–θ XRD patterns for LLT thin films on LSAT (100) substrates, fabricated at substrate temperature of 950 °C and oxygen pressure of 50 mTorr with different laser fluences.

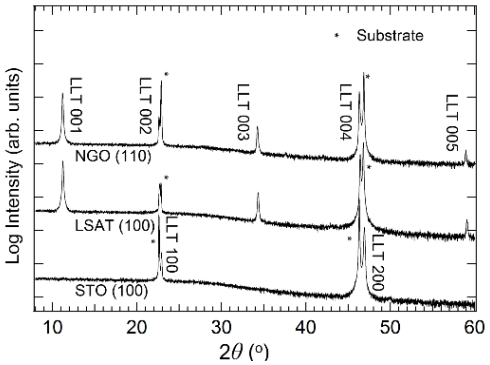

Figure 3 Out-of-plane 2θ–θ patterns of LLT epitaxial thin films fabricated under optimized condition.

Figure 3 shows out-of-plane 2θ-θ patterns of LLT thin films with a thickness of 120 nm on STO, LSAT and NGO substrates under optimized laser fluence of 1.4 J/cm^2, growth temperature of 950 °C, and oxygen pressure of 30 mTorr. The LLT thin film on STO (100) was oriented along *a*-axis since only LLT *h*00 appeared in the out-of-plane XRD

pattern, while those on LSAT (100) and NGO (110) substrates were *c*-axis oriented. Further analysis of in-plane LLT 101 peak indicates that the LLT thin film on STO is composed of two types of domains oriented perpendicular to each other, while those on LSAT and NGO were single domain. This difference in orientation can be explained by strain effect. The lattice constant relation between substrate and LLT can be described as $a_{STO} > c_{LLT}/2 \geq a_{LLT} > a_{LSAT} > a_{pNGO}$. On STO substrate, the *ac*-plane had smaller strain along the in-plane direction because of the tensile strain, resulting in *h*00 oriented LLT with domains containing two in-plane *c*-axis directions. On LSAT and NGO substrates, compressive strains were applied so that the *ab*-plane had smaller strain along the in-plane direction, and results in 00*l* orientation with single domain.

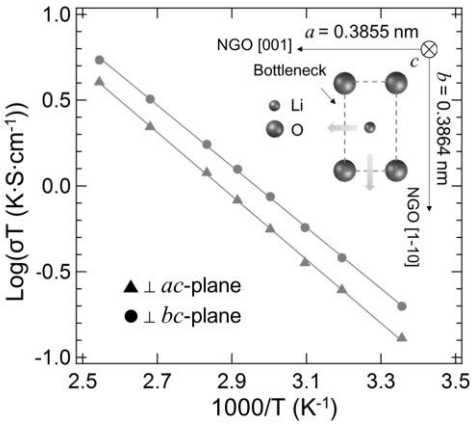

Figure 4 Arrhenius plot of in-plane ionic conductivity of LLT thin film across *ac*- and *bc*-planes. Inset shows schematic of Li ionic conduction across each bottleneck.

Reciprocal space mapping of epitaxial LLT thin film on each substrate indicates that the in-plane lattice constants of LLT thin films were exactly the same as those of the substrates, representing the coherent epitaxial growth and completely strained lattices. The lattice constant ranged from 0.3855 nm to 0.3905 nm, whose variation range is much wider than that of bulk LLT from 0.3872 nm to 0.3877 nm depending on Li composition. This result indicates that epitaxial strain has stronger influence on lattice cell size than chemical pressure.

Li ionic conductivity was measured for a 120 nm-thick LLT thin film on NGO substrate perpendicular to NGO [001] and NGO [1−10] directions. Since the LLT thin film was orthogonally strained by substrate, *a*- and *b*- axes are defined to describe the LLT direction along NGO [001] and NGO [1−10], thus a_p = 0.3855 nm and b_p = 0.3864 nm, same as correlated NGO axes respectively. In-plane Li ionic conductivity was measured in a temperature range of 298–393 K across two bottleneck *ac*- and *bc*- planes (Figure 4). The ionic conductivity at room temperature was observed as $\sigma_{298\,K}(ac)$ = 4.3 × 10^{-4} S/cm with activation energy $E_a(ac)$ = 0.36 eV across *ac*-plane, while $\sigma_{298\,K}(bc)$ was 6.7 × 10^{-4} S/cm with $E_a(bc)$ = 0.34 eV. Considering the lattice constant of bulk cubic $Li_{0.33}La_{0.56}TiO_3$ (a_p = 0.3875 nm), compressive strain of LLT along *a*-axis is larger than that along *b*-axis, resulting in a smaller bottleneck for Li ionic conduction path across *ac*-plane than that across *bc*-plane. This result indicates that stronger compressive strain results in a lower ionic conductivity and higher activation energy. This tendency is consistent with previous study using hydrostatic pressure [4]. It should be noted that this is the first time to observe strain-controlled ionic conduction in LLT under atmospheric condition. The present result demonstrates the artificial control of ionic conductivity through lattice strain.

3. Fabrication of epitaxial LSMO/LLT heterostructure and its interface

As discussed above, highly crystalline LLT was successfully formed, thus heteroepitaxial Li-ion battery cell structure can be fabricated. However, out-of-plane ionic conduction has scarcely been reported because epitaxially grown conductive bottom electrode is required. Therefore, such a heteroepitaxial structure was fabricated by choosing $La_{0.6}Sr_{0.4}MnO_3$ (LSMO) as a conductive bottom electrode and investigated the properties of LSMO/LLT interface. LSMO bottom electrodes were fabricated by PLD method with a stoichiometric $La_{0.6}Sr_{0.4}MnO_3$ target on STO, LSAT and

NGO substrates. LLT thin films were grown on LSMO buffer layers. Lattice and interface structures were evaluated by X-ray diffraction (XRD) and X-ray reflection (XRR).

The LSMO buffer layers on all substrates were 001 oriented with pseudo-cubic lattice. LLT layers were *a*-axis oriented on STO and *c*-axis oriented on LSAT/NGO, respectively. The thicknesses of the LSMO and LLT layers were 25 nm and 65 nm, respectively. Further analysis by reciprocal space mapping indicated that LSMO/LLT on STO was partially strain-relaxed while LSMO/LLT on LSAT and NGO had completely strained lattice. This proves that highly crystalline epitaxial heterostructures of LSMO/LLT were successfully fabricated, although their ionic conductivity was hardly measured.

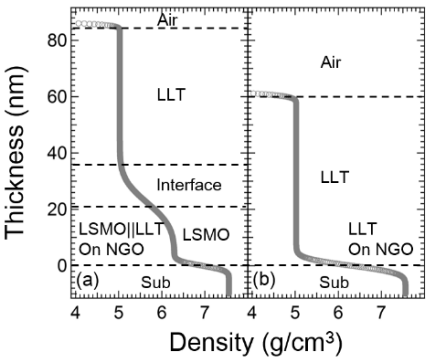

Figure 5 XRR fitting result of (a) LSMO/LLT and (b) LLT on NGO (110) substrate

Figure 5 shows XRR fitting result of LSMO/LLT and LLT on NGO substrate, manifesting the presence of thick and rough interface between LSMO and LLT. The LSMO/LLT interface has similar flatness to that of STO/LLT and LSAT/LLT, and is much thicker and rougher than that of NGO/LLT. This is probably due to the diffusion of Sr/La into LLT lattice through its A-site vacancy. The electrically conductive interface thus formed might lead to the failure in ionic conductivity measurement.

4. Summary

In this dissertation, strain engineering of phase pure LLT thin film with various orientations was demonstrated and LSMO/LLT heterostructure was fabricated by PLD method. High quality $Li_{0.33}La_{0.56}TiO_3$ epitaxial thin films were obtained by using a Li-rich target and by precisely controlling laser fluence. The in-plane ionic conductivity of LLT thin film on NGO (110) substrate was anisotropic and showed increasing activation energy under more compressive strain. The research on LLT thin films revealed that it is possible to control the orientation and ionic conductivity artificially under atmospheric conduction through epitaxial strain. High quality LSMO-buffered LLT heterostructure was successfully fabricated and its interface was studied in comparison with pure LLT thin film. Rough interface possibly due to Sr/La intermixing was observed. This study poses a new prospect for all solid state Li-ion battery structure.

Reference

[1] Y. Inaguma et al., *Solid State Commun.*, **1993**, *86*, 689-693

[2] T. Ohnishi et al., *Solid State Ionics*, **2012**, *228*, 80-82

[3] S. Kim et al., *CrystEngComm*, **2014**, *16*, 1044-1049

[4] Y. Inaguma et al., *J. Electrochem. Soc.*, **1995**, *142*, L8-L11